Synthesis and Magnetic Relaxation of $[Mn_{12}O_{12}(O_2CCH_2CH_2CH_2Cl)_{16}(H_2O)_4]$ Complex

WonSuk Jeon, Mi Kyung Jin, YooJin Kim, Duk-Young Jung,* Byoung Jin Suh,† and Seokwon Yoon†

Department of Chemistry-BK21 and the Institute of Basic Science, Sungkyunkwan University, Suwon 440-746, Korea
†Department of Physics, The Catholic University of Korea, Puchon 420-743, Korea
Received March 25, 2004

$Mn_{12}O_{12}(O_2CCH_2CH_2CH_2Cl)_{16}(H_2O)_4]$ (noted as Mn_{12}-BuCl), a new polynuclear complex of manganese chlorobutyrate has been successfully prepared by substitution of acetate with 4-chlorobutyric acid. The Mn_{12}-BuCl crystallizes into triclinic space group $P\bar{1}$ with a = 14.5560(11) Å, b = 14.5819(11) Å, c = 27.265(2) Å, α = 84.1140(10)°, β = 88.805(2)°, γ = 89.8820(10)°, and Z = 2. The local environments of manganese 3+ and 4+ ions of the title compound are close to those of other Mn_{12} compounds. The electrochemical data for Mn_{12}-BuCl involve reversible reactions of two-electron reductions. The Mn_{12}-BuCl also presents magnetic relaxation below 10 K implying that each molecule behaves as a single molecule magnet.

Key Words : Single-molecule magnets, Manganese, Magnetic relaxation, Chlorobutyric acid

Introduction

The nano-sized magnetic materials attracting great interests not only in industrial fabrication of high density information devices but also in understanding the magnetic properties of nano scale systems due to the gap between the quantum and classical magnetic mechanism.[1] Recently, single-molecule magnets (SMMs) are driving much interests thanks to well-defined magnetic molecules of nanometer size.[2] Several examples of SMMs have been reported, which contain manganese (Mn_{12} and Mn_4) and iron (Fe_8 and Fe_4) ions.[3] The slow magnetization relaxation of these compounds is evident, leading to unusual magnetic properties, for instance, steps in the magnetization hysteresis loop and frequency-dependent out-of-phase ac magnetic susceptibility signals.[4]

One of the most extensively studied SMMs is dodeca-nuclear manganese carboxylate complex, commonly called "Mn_{12}", $[Mn_{12}O_{12}(O_2CR)_{16}(H_2O)_4]\cdot$solv (R = Me, Et, CH_2Cl, Ph, CH_2Ph, C_6H_4-2-Br, C_6H_4-2-Cl and other complex ligands; solv = solvate molecules).[5] All the Mn_{12} compounds above Mn consist of twelve manganese ions, eight of the Mn in ring are in the +3 oxidation state (S = 2) and four in cubane are in the +4 state (S = 3/2), which give total S = 10 in the ground state. For Mn_{12} compounds, the source of the magnetic anisotropy arises from the molecules high-spin ground state combined with appreciable zero-field splitting.[6] Mn_{12} compounds show different magnetic properties depending on ligands utilized and synthetic conditions as observed in the previous Mn_{12}-PrCl compounds with different solvate molecules.[5j] So far the origin of the different rate of tunneling for the various Mn_{12} complexes is not clearly understood whether the different ground states, high order zero-field interaction, or other uncovered reasons present this phenomena as a critical parameter.

*Corresponding Author. Fax: +82-31-290-7075; e-mail: dyjung@skku.edu

In this paper we describe preparation, crystal structure and magnetic properties of a new SMM, $[Mn_{12}O_{12}(O_2CCH_2CH_2CH_2Cl)_{16}(H_2O)_4]$ (Mn_{12}-BuCl) to demonstrate the correlation of the crystal structure and the magnetic properties.

Experimental Section

All chemicals were obtained from Aldrich and used as received. $[Mn_{12}O_{12}(O_2CCH_3)_{16}(H_2O)_4]$ (denoted as Mn_{12}-Ac) was prepared by the method reported by Lis.[7] To a slurry of complex Mn_{12}-Ac (1.0 g, 0.5 mmol) in toluene (25 mL), 4-chlorobutyric acid (1.29 mL, 13.0 mmol) was added. The reaction mixture was stirred and solvent was evaporated under reduced pressure to remove acetic acid. The ligand exchange reaction using 4-chlorobutyric acid was repeated twice. The crystals of complex Mn_{12}-BuCl were grown in toluene/hexane and obtained by filtration, washed with hexane, and then dried in air.

Infrared (IR) spectra were obtained in 3600 to 400 cm^{-1} range by a Nicolet 205 FT-IR spectrometer. The sample was ground with dry KBr and pressed into a transparent disk. Elemental Analysis was performed by CE instruments EA1110 and ICP-MS was performed by VG Elemental PQ2 Turbo at the Inter-University Center of Natural Science Research Facilities in Seoul National University.

A black crystal of Mn_{12}-BuCl with dimensions 0.63 × 0.40 × 0.30 mm was mounted on a thin glass fiber. The diffraction data for single crystal of this compound were collected at 293 K using a SMART CCD diffractometer with graphite-monochromated Mo-Kα radiation (λ = 0.71073 Å). Cell parameters were determined and refined using the SMART[8] software, raw frame data were integrated using the SAINT programs, which corrects for Lorentz and polarization effects.[9] Empirical absorption correction was applied with the program SADABS.[10] The structure was solved by direct methods (SHELX-86) and the standard difference Fourier techniques (SHELX-97).[11] All non-hydrogen atoms were

Table 1. Crystal data and structure refinement for Mn_{12}-BuCl

Identification code	$[Mn_{12}O_{12}(OOCCH_2CH_2CH_2Cl)_{16}(H_2O)_4]2CH_3C_6H_5$
Empirical formula	$C_{78}H_{120}Cl_{16}Mn_{12}O_{48}$
Formula weight	3054.22
Temperature	173(2) K
Wavelength	0.71073 Å
Crystal system	triclinic
Space group	*P*-1
Unit cell dimensions	*a* 14.5560(11) Å *α* 84.1140(10)°
	b 14.5819(11) Å *β* 88.805(2)°
	c 27.265(2) Å *γ* 89.8820(10)°
Volume	5755.4(7) Å
Z	2
Density (calculated)	1.733 Mg/m^3
Absorption coefficient	1.723 mm^{-1}
F(000)	3016
Crystal size	$0.63 \times 0.40 \times 0.30$ mm^3
θ range for data collection	1.40 to 28.30 °
Index ranges	$-18 \le h \le 11$, $-19 \le k \le 19$, $-34 \le l \le 35$
Reflections collected	35580
Independent reflections	25839 [R(int) 0.0265]
Refinement method	Full-matrix least-squares on F^2
Data / restraints / parameters	25839 / 0 / 1369
Goodness-of-fit on F^2	1.041
Final R indices [$I>2\sigma(I)$]	*R* 0.0811, R_w 0.2143
R indices (all data)	*R* 0.1037, R_w 0.2311
Largest diff. peak and hole	2.612 and -2.785 $e.Å^3$

refined anisotropically. All hydrogen atoms were calculated at idealized positions. The hydrogen on coordinated water molecule was refined separately according to electron density difference but those of non-coordinated water were not refined.

Three intense reflections were monitored every 200 reflections to check stability. Anisotropic thermal parameters for all non-hydrogen atoms were included in the refinements. The full-matrix least-squares refinement finally converged with $R1 = 0.0811$ (based on F) and $wR2 = 0.2143$ (based on F^2) for observed reflections ($F_o > 4\sigma(F_o)$). The crystallographic data including conditions of data collection, are summarized in Table 1.

Electrochemical studies were performed by a BAS 100W voltammetric analyzer and a standard three-electrode assembly (glassy carbon working, Pt plate auxiliary and Ag/AgCl reference) with 0.1M $NBu^n_4PF_6$ as supporting electrolyte. Quoted potential values are versus the ferrocene/ferrocenium couple measured under the same conditions. The scan rate for cyclic voltammetry and differential pulse voltammetry was set at 100 and 20 mV/s, respectively. The concentration of the measured solutions was approximately 1 mM. As solvents, CH_2Cl_2 for Mn_{12}-PrCl and Mn_{12}-BuCl was used and CH_3CN for Mn_{12}-Ac, respectively.

Variable temperature direct current (dc) and alternating current (ac) magnetic susceptibility measurements were carried out on a Quantum Design MPMS 7 and PPMS 5 SQUID magnetometers with an applied magnetic field of 100 Gauss in the temperature range of 2-300 K.

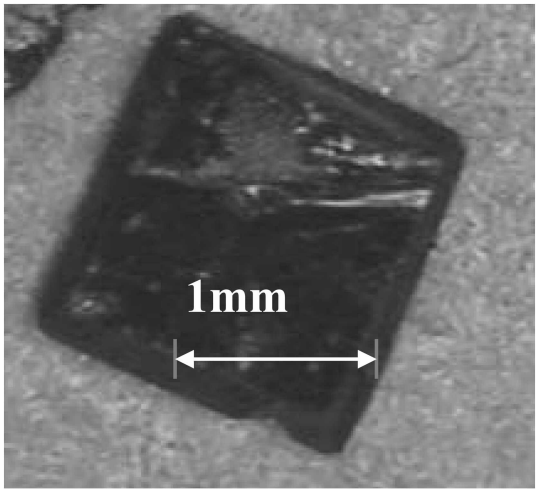

Figure 1. Optical microscopic photo of a single crystal sample of Mn_{12}-BuCl.

Results and Discussion

Synthesis. Crystal samples of Mn_{12}-BuCl were obtained as parallelepiped shapes and the biggest one has 2 millimeter edge length as shown in Figure 1. Polycrystalline samples of Mn_{12}-BuCl are soluble in CH_2Cl_2 and are stable in various organic solutions in aerobic condition at least for a week. Analysis: calculated for $C_{78}H_{120}Cl_{16}Mn_{12}O_{48}$: C 28.50; H 3.90; Mn 21.50%; found: C 27.40; H 3.80; Mn 20.90%. The IR spectra for Mn_{12}-BuCl present the band in the vicinity of 1580 cm^{-1} assigned as $(OCO)_{asym}$, which implies metal-carboxylate complex formation through the carboxyl group

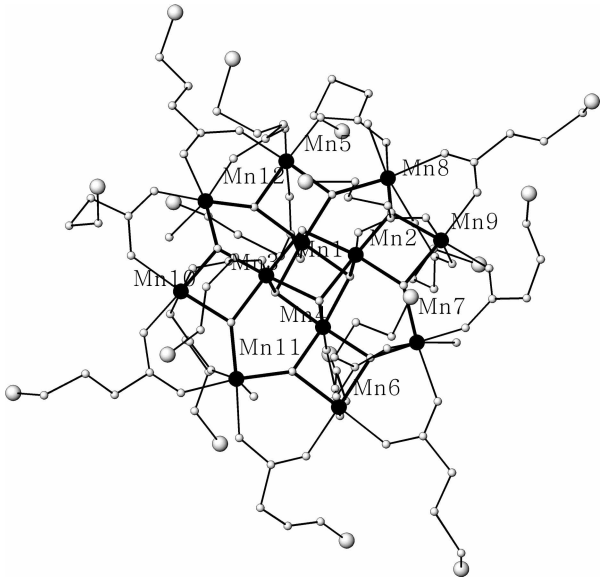

Figure 2. Molecular structure of Mn_{12}-BuCl. Ellipsoids are drawn for 50% probability, and hydrogen atoms have been omitted for clarity.

Table 2. Bond distances (Å) between manganese and oxygen of Mn_{12}-BuCl

Mn (oxidation state)	axial	equatorial				
Mn1(IV)	1.901	1.885	1.881	1.855	1.912	1.903
Mn2(IV)	1.892	1.874	1.876	1.848	1.901	1.941
Mn3(IV)	1.904	1.882	1.881	1.841	1.939	1.907
Mn4(IV)	1.891	1.890	1.846	1.890	1.915	1.935
Mn5(III)	2.204	2.170	1.934	1.954	1.883	1.901
Mn6(III)	2.147	2.206*	1.970	1.987	1.886	1.881
Mn7(III)	2.178	2.204	1.922	1.946	1.902	1.878
Mn8(III)	2.104	2.173*	1.960	1.983	1.886	1.883
Mn9(III)	2.177	2.183	1.909	1.947	1.896	1.915
Mn10(III)	2.110	2.193*	1.982	1.992	1.874	1.881
Mn11(III)	2.188	2.207	1.932	1.910	1.883	1.885
Mn12(III)	2.086	2.162*	1.953	1.991	1.894	1.881

*oxygen atoms from coordinated water molecules.

since free carboxylic acids give bands in around 1700 cm^{-1}.[12]

Crystal Structure. Mn_{12}-BuCl crystallize in the triclinic space group *P*-1 and contain discrete $[Mn_{12}O_{12}(O_2CCH_2CH_2CH_2Cl)_{16}(H_2O)_4]$ molecules as shown in Figure 2. Overall, the structure of Mn_{12}-BuCl almost superposes on Mn_{12}-PrCl and involves lower symmetric packing than that of Mn_{12}-Ac.[7] The inner core $[Mn(IV)_4O_4]^{8-}$ cubane unit is held within a non-planar ring of eight Mn(III) atoms by eight μ_3-oxide atoms. Outer Mn(III) ($3d^4$) atoms show a Jahn-Teller (J-T) distortion with an elongation along the axes approximately parallel to the unique molecular C_2 axis. The four water molecules on four Mn(III) are all on J-T axial sites, and their bond lengths are similar to the axial Mn-O(carboxylato) values as summarized in Table 2. It should

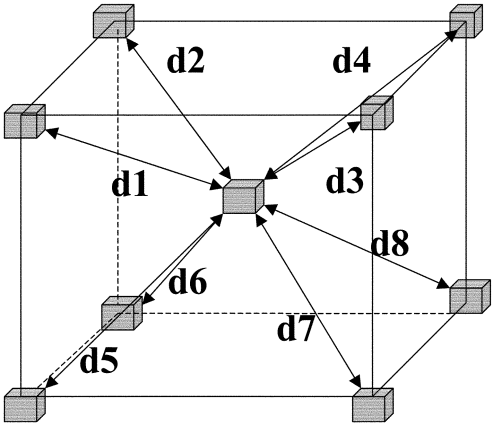

Figure 3. Molecular packing and distances between nearest molecules in Mn_{12}-compounds.

be noted that the Mn_{12}-BuCl has the binding sites of water and carboxylate group same as those of the Mn_{12}-Ac and Mn_{12}-PrCl. The structural isomers according to the different position of coordinated water molecules were not observed in the present study.[13] The distances between the nearest eight other complexes in the Mn_{12}-BuCl and other Mn_{12}-compounds were calculated based on the crystallographic data as shown in Figure 3. Mn_{12}-Ac: 8 × 13.72 Å, Mn_{12}-PrCl(1): 13.07, 13.12, 13.27, 13.31, 14.78, 15.40, 19.24, 19.66 Å, Mn_{12}-PrCl(2): 12.92, 13.19, 13.51, 13.72, 15.62, 15.80, 19.70, 20.30, Mn_{12}-BuCl: 16.12, 16.14, 16.87, 16.89, 17.74, 17.74, 18.42, 18.42 Å. Interestingly, the variation of the inter-complex distances in Mn_{12}-BuCl is smaller than those of Mn_{12}-PrCl compounds. Both Mn_{12}-PrCl compounds involve four short, two moderate and two short distances. The average values for Mn_{12}-PrCl(1) and Mn_{12}-PrCl(2) are 15.23 and 15.60', respectively.

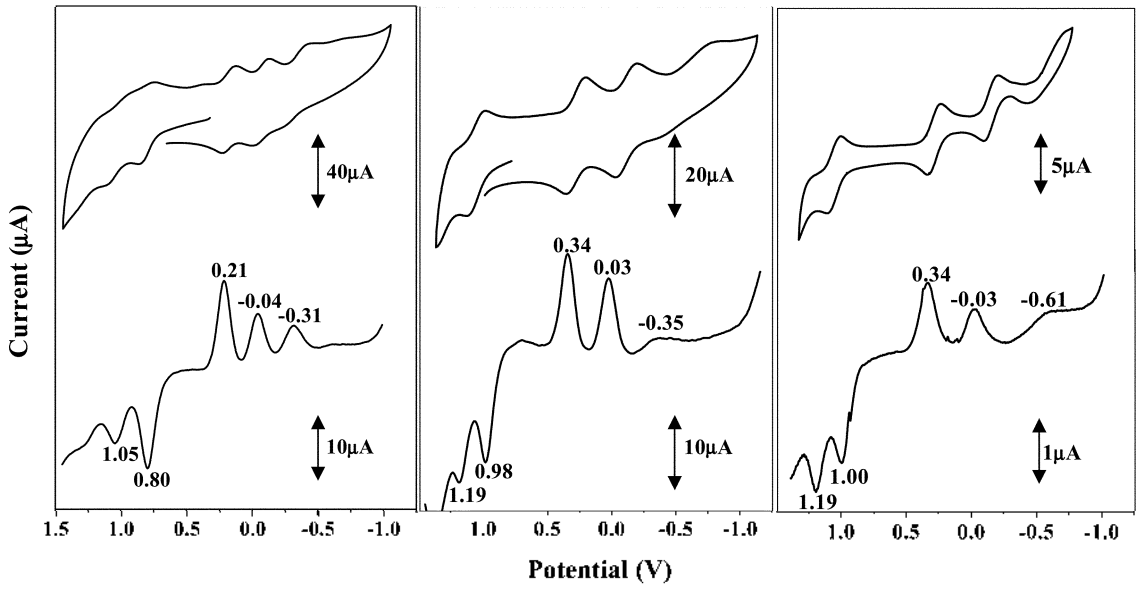

Figure 4. Cyclic voltammogram (top) and differential pulse voltammogram (bottom) of Mn_{12}-compounds. The potentials are given versus the ferrocene/ferrocenium couple measured under the same conditions except for the solvents. (a) Mn_{12}-acetate. (b) Mn_{12}-PrCl and (c) Mn_{12}-BuCl.

Electrochemistry. Cyclic voltammetry (CV) and differential pulse voltammetry (DPV) provide electrochemical properties and characteristics of the prepared compounds and also give insight into any complicating side processes such as pre- and post-electron-transfer reaction. In Figure 4, the CV and DPV data for the selected Mn_{12}-compounds in CH_2Cl_2 or CH_3CN solution are plotted. For Mn_{12}-BuCl, there are several redox couples apparent, three on the reduction side and two on the oxidation side. Three of the redox couples appear to be reversible or quasi-reversible, the first reduction at 0.34 V, the second reduction at -0.03 V, and the first oxidation process at 1.00 V, respectively.

$$[Mn_{12}O_{12}]^{2+} \leftarrow [Mn_{12}O_{12}]^{+} \leftrightarrow [Mn_{12}O_{12}]^{0} \leftrightarrow [Mn_{12}O_{12}]^{-} \leftrightarrow [Mn_{12}O_{12}]^{2-} \rightarrow [Mn_{12}O_{12}]^{3-} \quad (1)$$

For these ones, the forward and reverse waves are well formed with a peak separation (180 mV) comparable to that of ferrocene under the same conditions. The peak separations for other redox couples, the third reduction and the second oxidation, are much larger than those for the reversible ones, where the DPV scans show broader, ill-formed peaks in contrast to the shaper, better-formed peaks for the reversible ones. The electrochemical data for the selected Mn_{12}-compounds are summarized in Table 3. In order to compare other electrochemical data, the measurements for Mn_{12}-Ac have been carried out, resulting in the first oxidation and reduction for Mn_{12}-Ac of 0.80 V and 0.21 V, close to those values (0.82 V and 0.19 V) reported by Hendrickson *et al.*[5c] The electrochemical potentials of the first oxidation and reduction waves depend on the response to the electronic properties of the carboxylate. The electronegative carboxylate causes to reduce the electron density on the metal cluster and thereby makes the cluster easier to be reduced and harder to be oxidized.[5d] The chlorines in chlorobutyrate ligands make the Mn_{12} cluster difficult to be reduced and facile to be oxidized compared with Mn_{12}-Ac. The influence of chlorine atoms in 3-chloropropyl and 4-chlorobutyric ligands upon the redox properties are similar each other and smaller than that of chloromethyl ligands. Generally, electron donating substituent of propyl or butyl groups causes the carboxylate to become more basic, enhancing the electron density on the metal cluster. However, electronegative chlorine is predominant factor determining the redox properties in Mn_{12}-compounds when we assume the solvent effect is very negligible. It should be also noted that the relatively large values of the first and the second reductions for the Mn_{12}-BuCl and Mn_{12}-PrCl open the preparation of mono-anionic members of the Mn_{12} family by one-electron reduction of the neural clusters.

Table 3. Electrochemical data[a] for selected $[Mn_{12}O_{12}(O_2CR)_{16}(H_2O)_4]$

R in Mn_{12} compounds	reduction ($E_{1/2}$)			oxidation ($E_{1/2}$)		reference
	3rd	2nd	1st	1st	2nd	
CH_3 [b]	-0.31	-0.04	0.21[d]	0.80[d]	1.05	this work
CH_3 [b]	-0.35	-0.07	0.19	0.82		[5d]
CH_2CH_3 [c]		-0.50	0.02	0.79	1.03	[5d]
$(CH_2)_{16}CH_3$ [c]	-0.80	-0.39	0.04[d]	0.75		[5k]
CH_2Cl [b]		0.30	0.60			[5l]
$CHCl_2$ [b]		0.61	0.91			[5l]
CH_2CH_2Cl [c]	-0.35	0.03[d]	0.34[d]	0.98[d]	1.19	this work
$(CH_2)_2CH_2Cl$ [c]	-0.61	-0.03[d]	0.34[d]	1.00[d]	1.19	this work
C_6H_5 [c]		-0.23	0.12	0.82	1.16	[5d]
C_6F_5 [b]		0.46	0.64			[5l]

[a]Potential were obtained from DPV scans and are given in volts *vs* the ferrocene/ferrocenium couple. [b]$CH_3C{\equiv}N$ is used as a solvent in the measurements. [c]CH_2Cl_2 is used as a solvent in the measurements. [d]reversible reaction observed in this study.

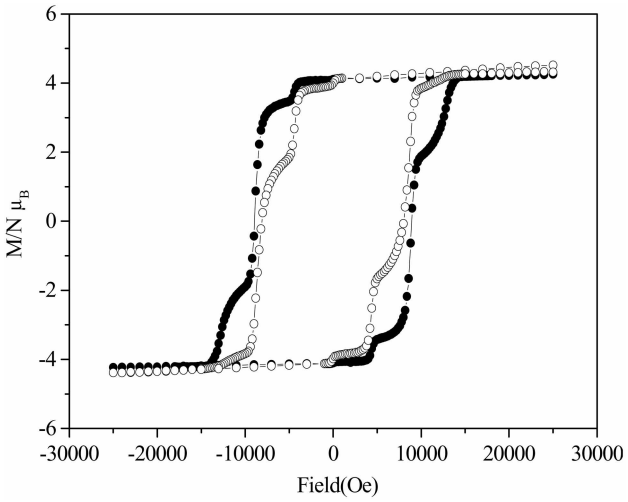

Figure 5. Magnetization hysteresis loops measure at 2.15 K (●) and 2.30 K (○) for oriented crystals in eicosane matrix for Mn_{12}-BuCl.

Magnetic properties. Mn_{12}-BuCl exhibits a hysteresis loop at 2.15 and 2.30 K, as shown in Figure 5. The measurement was performed after the sample has been cooled to 2 K in zero field. After thermal equilibration, the

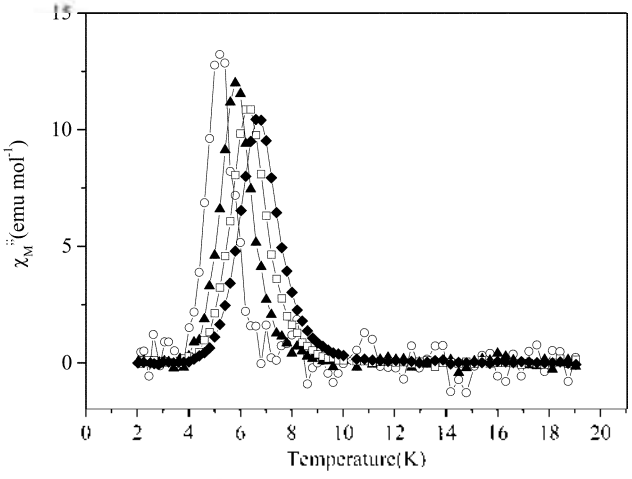

Figure 6. Plot of out-of-phase ac magnetic susceptibility χ_M'' *vs.* temperature for the single crystal samples of Mn_{12}-BuCl. Data were collected with zero dc magnetic field and with an 1.0 G ac field oscillating at: 50 Hz (○), 200 Hz (▲), 500 Hz (□) and 1000 Hz (◆).

magnetization was measured as the magnetic field was increased to 30.0 kG, decreased to zero, reversed in direction to -30.0 kG and then returned to zero. A large magnetic anisotropy of Mn_{12} clusters cause to the hysteresis loop for Mn_{12}-BuCl, which involves several steps resulting from the magnetization tunneling, similar with that for Mn_{12}-PrCl.[14]

Out-of-phase ac magnetic susceptibility (χ_M'') data are measured for Mn_{12}-BuCl complex in the region 1.9 to 19 K, at different frequencies in zero field (Figure 6), which exhibit frequency-dependent ac χ_M'' peaks in the region 4 to 8 K, demonstrating Mn_{12}-BuCl complex behave as SMMs. It should be noted that the peaks in the range between 2 to 4 K were not observed.

Conclusion

Various chemical analyses showed that a new Mn_{12}-compound, Mn_{12}-BuCl was successfully synthesized as single crystals. The electrochemical properties of the title compound open the new Mn_{12}-complexes such as one- and/or two-electron reduced complexes, which have different total magnetic spin values. The magnetic hysteresis loop of Mn_{12}-BuCl shows several steps, which indicates magnetization tunneling of Mn_{12} cluster complexes.

Acknowledgments. This work was supported by the KOSEF (R01-2003-000-10849-0). The Korea Basic Science Institute provided us with SQUID magnetometer measurements. DYJ thanks the Faculty Research Fund, Sungkyunkwan University.

Supplementary Materials. Crystallographic data for the structure reported here have been deposited with the Cambridge Crystallographic Data Center (Deposition No. CCDC-239927). That data can be obtained free of charge via (or from the CCDC, 12 Union Road, Cambridge CB2 1EZ, UK; fax: +44 1223 336033; e-mail: deposit@ccdc.cam.ac.uk)

References

1. (a) Awschalom, D. D.; Di Vincenzo, D. P. *Phys. Today* **1995**, *48*, 43. (b) Awschalom, D. D.; Di Vincenzo, D. P.; Smyth, J. F. *Science* **1992**, *258*, 414. (c) Leslie-Pelecky, D. L.; Rieke, R. D. *Chem. Mater.* **1996**, *8*, 1770. (d) Tejada, J.; Ziolo, R. F.; Zhang, X. X. *Chem. Mater.* **1996**, *8*, 1784.
2. Christou, G.; Gatteschi, D.; Hendrickson, D. N.; Sessoli, R. *MRS Bulletin* **2000**, *25*, 66.
3. Gatteschi, D.; Sessoli, R. *Angew. Chem., Int. Ed.* **2003**, *42*, 268.
4. (a) Sessoli, R.; Gatteschi, D.; Caneschi, A.; Novak, M. A. *Nature* **1993**, *365*, 141. (b) Friedman, J. R.; Sarachik, M. P.; Tejada, J.; Ziolo, R. *Phys. Rev. Lett.* **1996**, *76*, 3830. (c) Thomas, L.; Lionti, F.; Ballou, R.; Gatteschi, D.; Sessoli, R.; Barbara, R. *Nature* **1996**, *383*, 145.
5. (a) Caneschi, A.; Gatteschi, D.; Sessoli, R.; Barra, A. L.; Brunel, L. C.; Guillot, M. *J. Am. Chem. Soc.* **1991**, *113*, 5873. (b) Boyd, P. D. W.; Li, Q.; Vincent, J. B.; Folting, K.; Chang, H.-R.; Streib, W. E.; Huffman, J. C.; Christou, G.; Hendrickson, D. N. *J. Am. Chem. Soc.* **1988**, *110*, 8537. (c) Sessoli, R.; Tsai, H.-L.; Schake, A. R.; Wang, S.; Vincent, J. B.; Folting, K.; Gatteschi, D.; Christou, G.; Hendrickson, D. N. *J. Am. Chem. Soc.* **1993**, *115*, 1804. (d) Eppley, H. J.; Tsai, H.-L.; de Vries, N.; Folting, K.; Christou, G.; Hendrickson, D. N. *J. Am. Chem. Soc.* **1995**, *117*, 301. (e) Aubin, S. M. J.; Sun, Z.; Guzei, I. A.; Rheingold, A. L.; Christou, G.; Hendrickson, G. N. *Chem. Commun.* **1997**, 2239. (f) Wei, Y.-G.; Zhang, S.-W.; Shao, M.-C.; Tang, Y.-Q. *Polyhedron* **1997**, *16*, 1471. (g) Ruiz, D.; Sun, Z.; Albela, B.; Folting, K.; Ribas, J.; Christou, G.; Hendrickson, D. N. *Angew. Chem., Int. Ed.* **1998**, *37*, 300. (h) Sun, Z.; Ruiz, D.; Rumberger, E.; Incarvito, C. D.; Folting, K.; Rheingold, A. L.; Christou, G.; Hendrickson, D. N. *Inorg. Chem.* **1998**, *37*, 4758. (i) An, J.; Chen, Z.-D.; Bian, J.; Chen, J.-T.; Wang, S.-X.; Gao, S.; Xu, G.-X. *Inorg. Chim. Acta* **2000**, *299*, 28. (j) Park, C. D.; Rhee, S. W.; Kim, Y. J.; Jeon, W. S.; Jung, D. Y.; Kim, D. H.; Do, Y.; Ri, H. C. *Bull. Korean Chem. Soc.* **2001**, *22*, 453. (k) Park, C. D.; Jung, D. Y. *Bull. Korean Chem. Soc.* **2001**, *22*, 611. (l) Soler, M.; Chandra, S. K.; Ruiz, D.; Davidson, E. R.; Hendrickson, D. N.; Christou, G. *Chem. Commun.* **2000**, 2417.
6. (a) Schwarzschild, B. *Phys. Today* **1997**, *50*, 17. (b) Chudnovsky, E. M. *Science* **1996**, *274*, 938. (c) Caneschi, A.; Ohm, T.; Paulsen, C.; Rovai, D.; Sangregorio, C.; Sessoli, R. *J. Magn. Magn. Mater.* **1998**, *177*, 1330. (d) Caneschi, A.; Gatteschi, D.; Sangregorio, C.; Sessoli, R.; Sorace, L.; Cornia, A.; Novak, M. A.; Paulsen, C.; Wernsdorfer, W. *J. Magn. Magn. Mater.* **1999**, *200*, 182.
7. Lis, T. *Acta Crystallogr. Sec. B* **1980**, *36*, 2042.
8. *SMART*, version 5.0; data collection software; Bruker AXS, Inc.; Madison, WI, 1998.
9. *SAINT*, version 5.0; data integration software; Bruker AXS, Inc.; Madison, WI, 1998.
10. *Sheldrick, G. M. SADABS. A program for absorption correction with the Bruker SMART system*; Universitat Göttingen: Göttingen, Germany, 1996.
11. McArdle, P. *SHELX-86 and SHELX-97 Users Guide*; Crystallography Center, Chemistry Department, National University of Ireland: Galway, Ireland; *J. Appl. Crystallogr.* **1995**, *28*, 65.
12. (a) Nakamoto, K. *Infrared and Raman Spectra of Inorganic and Coordination Compounds*; 5th Ed; John Wiley & Sons: New York, 1997; pp 59-62. (b) Mehrotra, R. C.; Bohra, R.; *Metal Carboxylates*; Academic Press Inc.: New York, 1983; pp 48-60. (c) Lee, Y. K.; Lee, S. W. *Bull. Korean Chem. Soc.* **2003**, *24*, 906.
13. Aubin, S. M. J.; Sun, Z.; Eppley, H. J.; Rumberger, E. M.; Guzei, I. A.; Folting, K.; Gantzel, P. K.; Rheingold, A. L.; Christou, G.; Hendrickson, D. N. *Inorg. Chem.* **2001**, *40*, 2127.
14. (a) Heu, M.; Suh, B. J.; Yoon, S.; Jeon, W. S.; Kim, Y. J.; Jung, D. Y. *J. Korean Phys. Soc.* **2003**, *43*, 544. (b) Yoon, S. W.; Heu, M.; Jeon, W. S.; Jung, D. Y.; Suh, B. J.; Yoon, S. *Phys. Rev. B* **2002**, *67*, 52402.